

# Implication of VEGF and aquaporin 4 mediating Müller cell swelling to diabetic retinal edema

Teruyo Kida<sup>1</sup> · Hidehiro Oku<sup>1</sup> · Taeko Horie<sup>1</sup> · Masanori Fukumoto<sup>1</sup> · Yoshitaka Okuda<sup>1</sup> · Seita Morishita<sup>1</sup> · Tsunehiko Ikeda<sup>1</sup>

Received: 3 November 2016 / Revised: 13 February 2017 / Accepted: 6 March 2017 / Published online: 16 March 2017  
© Springer-Verlag Berlin Heidelberg 2017

## Abstract

**Purpose** Aquaporin 4 (AQP4), a water channel protein, is known to be expressed in retinal Müller cells. The purpose of this study was to determine the effects of VEGF and AQP4 channels on the volumetric changes in Müller cells.

**Methods** Retinas from diabetic rats and a cultured Müller cell line, TR-MUL5, were used in this study. Intravitreal injections of VEGF or PBS were performed on either streptozotocin (STZ)-induced diabetic or normoglycemic rats. Retinal sections were immunostained for anti-gial fibrillary acidic protein (GFAP), anti-AQP4, and anti-VEGF. VEGF protein levels from collected retinas were determined by western blot analysis. Volumetric changes and nitric oxide (NO) levels in cultured Müller cells were determined using flow cytometry (FACS), in the presence or absence of VEGF and TGN-020, a selective AQP4 inhibitor.

**Results** In the diabetic rat retina, VEGF immunoreactivity was concentrated in the internal retinal layers, and AQP4 immunoreactivity was higher than controls. The expressions of AQP4 were colocalized with GFAP. Protein levels of VEGF in the hyperglycemic rat retina were significantly higher than controls. FACS analyses showed that exposure to VEGF enlarged Müller cells, while exposure to TGN-020 suppressed the enlargement. Intracellular levels of NO were increased after exposure to VEGF, which was suppressed following the addition of TGN-020.

**Conclusion** The observed Müller cell swelling is mediated by VEGF and AQP4.

**Keywords** Aquaporin 4 · VEGF · Müller cell · Retinal edema · Streptozotocin (STZ) induced hyperglycemic rat

## Introduction

Diabetic retinopathy is a leading cause of blindness, which is due to two major vision-threatening clinical conditions; proliferative retinopathy and macular edema [1–3]. Metabolic control remains the most effective means of controlling diabetic retinopathy and other diabetes-related complications; however, diabetic macular edema (DME) develops even at the early stages of diabetic retinopathy.

Chronic increase of blood glucose levels leads to an upregulation of vascular endothelial growth factor (VEGF), which results in the breakdown of the inner and outer blood retinal barriers [4, 5]. The pathological roles VEGF plays in causing retinal edema have been elucidated, [6] and anti-VEGF therapy, which blocks the action of VEGF, is widely used for treatment of DME [7, 8]. Inhibition of VEGF rapidly reduces macular edema in eyes with diabetic retinopathy, even in patients with poor metabolic control; however, repeat injections are often required due to the recurrence of macular edema.

Müller cells are the primary glial cells of the retina. They extend longitudinally through the retina from the outer nuclear layer to the border of the retina and vitreous [9]. Aquaporin 4 (AQP4), a water channel protein, [10] is known to be expressed in retinal Müller cells [11, 12]. These water channel proteins are densely packed at the footplates of Müller cells and their processes surrounding retinal blood vessels in the superficial and deep vascular plexus [13]. Because AQP4 is closely associated with the formation and resolution of brain edema, [14]. Müller cells are likely to be the main conductor of water and ionic homeostasis in the retina. It has been

✉ Teruyo Kida  
kidateruyo@gmail.com

<sup>1</sup> Department of Ophthalmology, Osaka Medical College, 2-7 Daigaku-machi, Takatsuki, Osaka 569-8686, Japan

suggested that AQP4 deletion is neuroprotective against ischemic retinal injuries [15].

AQP4 can also act as a reservoir for nitric oxide (NO) molecules and can control NO flow in the central nervous system (CNS) [16]. Additionally, NO can act on AQP4 channels and alter the water permeability of astrocytes [17]. VEGF is known to increase NO formation in the brain [18, 19]. Thus, we hypothesized that VEGF may cause swelling of Müller cells via regulation of the AQP4 channel, which results in retinal edema. To test our hypothesis, immunoblot analysis was performed to determine whether the expression of VEGF was increased in the retina of streptozotocin (STZ)-induced diabetic rats. Immunohistochemistry was also performed to determine the expression of VEGF, AQP4, and GFAP in the diabetic retina. Additionally, we used flow cytometry to determine whether VEGF increases cellular volume of cultured TR-MUL5 cells, a Müller cell line, in the absence or presence of TGN-020, an AQP4-channel blocker and DAF-2DA (4,5-diaminofluorescein diacetate), a fluorescent probe for NO.

## Materials and methods

### Animals

Twenty-eight, nine-week-old male Wistar rats weighing between 180 and 200 g were purchased from Japan SLC Inc. (Shizuoka, Japan) and housed in an air-conditioned room at a temperature of approximately 23°C with a humidity of 60%. They were maintained on a 12-hour light/dark cycle and received food and water ad libitum. They were handled in accordance with the ARVO Statement for the Use of Animals in Ophthalmic and Vision Research. Our experimental protocols conformed to the Animal Research: Reporting In Vivo Experiments (ARRIVE) guidelines [20] and was approved by the Osaka Medical College Committee on the Use and Care of Animals (Approval number: 27114).

### Chemicals

All chemicals were obtained from Sigma-Aldrich (St. Louis, MO, USA), unless otherwise specified.

### Anesthesia and euthanasia

All procedures were performed under general anesthesia via intraperitoneal injection of medetomidine (0.75 mg/kg), midazolam (4 mg/kg), and butorphanol (5 mg/kg). Rats were euthanized by exposure to CO<sub>2</sub> at a rate of 6 L/min in a 13.8 L cage with wood shaving bedding.

### Induction of diabetes

To induce diabetes, each animal received a single 60 mg/kg intraperitoneal injection of streptozotocin in 10 mM sodium citrate buffer, pH 4.5, after an overnight fast while under general anesthesia. As controls, nondiabetic animals received an injection of citrate buffer alone. Animals with blood glucose levels higher than 250 mg/dL 24 hours after injections were considered diabetic. All experiments were conducted 2 weeks after the induction of diabetes.

### Intravitreal injection

Two microliter intravitreal injections of VEGF (10 ng/μl) (recombinant human VEGF<sub>165</sub>, R&D Systems, Inc., Minneapolis, MN, USA) in PBS or vehicle alone (PBS) were performed using a Hamilton syringe and a 30-gauge needle. Animals received general anesthesia as previously described, and perfused fixation was performed 24 hours after the intravitreal injections.

### Immunohistochemistry of retinal slices

Sixteen rats were deeply anesthetized and perfused through the heart with saline followed by 4% paraformaldehyde (PFA) in 0.1 M phosphate buffer saline, pH 7.4. The retinas were carefully removed and post-fixed in 4% PFA in PBS overnight. After washing with PBS, the retinal tissues were immersed in 30% sucrose overnight at 4°C and then embedded in OCT compound (Sakura Finetechnical, Tokyo, Japan). Then, 10 μm frozen sections were cut with a cryostat. After blocking with 1% normal goat serum plus 1% BSA and 0.1% triton X-100 in PBS, the retinal sections were incubated overnight at 4°C with the following primary antibodies: mouse monoclonal anti-GFAP (1:500), rabbit polyclonal anti-AQP4 (1:500), and VEGF (1:500, Santa Cruz Biotechnology, Inc., Dallas, TX, USA). The processed sections were photographed with a fluorescent microscope (BZ-X700, Keyence, Osaka, Japan).

### Protein levels of VEGF in retinal slices by western blot

Retinas were excised from the eyes and homogenized in lysis buffer containing 1 mM phenyl methanesulfonyl fluoride, 10 μM pepstatin A, 10 μM leupeptin, 10 μM aprotinin, 0.1% sodium dodecyl sulfate (SDS), 1% Nonidet P-40, 5% sodium deoxy cholate, 50 mM Tris-HCl (pH 7.6), and 150 mM sodium chloride. The suspension was centrifuged, and the total protein concentration of the resulting supernatant was determined using the Lowry method (DC Protein Assay Reagent, Bio-Rad, Hercules, CA, USA). Samples were separated on a 12% SDS-polyacrylamide gel and blotted onto PVDF membranes. The membranes were then blocked with 5% skim milk in Tris-buffered saline, pH 7.4 with 0.1%

Tween 20 (TBS-T) followed by an overnight incubation at 4°C with a rabbit polyclonal antibody (1:1000) against VEGF (147) (sc-507, Santa Cruz, Dallas, USA). Tubulin ( $\alpha$ -tubulin, 1:1000; Merck Millipore, CP06) was used as an internal control. The membranes were washed three times in TBS-T followed by incubation with a peroxidase-conjugated goat anti-rabbit IgG (1:2500, Promega, Madison, WI, USA) secondary antibody for 2 hours at 37°C. The protein bands were visualized following the addition of an ECL Plus western blotting detection system (GE Healthcare, Little Chalfont, UK). Protein band densities were measured with a luminescent image analyzer (LAS-3000, Fujifilm, Tokyo, Japan). Relative protein levels were quantified using the embedded software (Multi Gauge version 3.0) and standardized according to  $\alpha$ -tubulin protein levels.

### Cell cultures

A rat retinal Müller cell line, TR-MUL5, was obtained from Fact, Inc. (Sendai, Japan) [21]. These cells were collected from transgenic rats carrying a temperature-sensitive SV40 large T-antigen gene [21, 22]. The TR-MUL5 cells were cultured in Dulbecco's Modified Eagle's Medium (DMEM) supplemented with 10% fetal bovine serum (FBS) at 33°C in a humidified atmosphere of 5% CO<sub>2</sub>/air. Before reaching confluence, the temperature was raised to 37°C in order to arrest the proliferation by reducing the expression of the large T-antigen. Additionally, the media was changed to a control DMEM media containing a physiological concentration of 5.5 mM glucose. The TR-MUL5 cells were then cultured in control mediums lacking 10% FBS and serum-deprived overnight. TR-MUL5 cells at passages 18 and 19 were used in this study. Detailed procedures and treatment protocols for each experiment are described later.

### Measurement of intracellular levels of NO and cell volume by flow cytometry (FACS)

To examine the effect of VEGF on the volume of cultured Müller cells (TR-MUL5), the cells were incubated in the presence or absence of VEGF (5 ng/mL) overnight. Then, the cells were harvested via trypsinization and centrifuged at 800 x g for 5 minutes. The cells were resuspended in phenol red-free DMEM with 5  $\mu$ M 4,5-diaminofluorescein diacetate (DAF-2DA; Cayman, Ann Arbor, MI, USA) for another 20 minutes at 37°C. Cell densities were adjusted to  $2.0 \times 10^5$  cells/mL and incubated in the presence or absence of 100 nM TGN-020 for 30 minutes at 37°C.

Increased water permeability through AQP4 channels can cause volumetric changes within the cells due to osmotic stress. Thus, after washing with PBS, the cells were resuspended in a hypotonic solution. The hypotonic solution (60% osmolarity) was made by adding distilled water to an extracellular solution

consisting of 136 mM NaCl, 3 mM KCl, 2 mM CaCl<sub>2</sub>, 1 mM MgCl<sub>2</sub>, 10 mM HEPES, 11 mM glucose at pH 7.4, and an osmolality adjusted to 180 mOsm, which is normally 300 mOsm [23].

Because the change in impedance, as determined by flow cytometry, is proportional to the cellular volume, the cellular volume was determined by the relative changes in impedance during the sample acquisition [24]. Addition of DAF-2DA enabled us to determine the changes of intracellular NO levels simultaneously. Thus, the changes in the intracellular levels of NO and cellular volume of Müller cells were analyzed using flow cytometry (EC800, SONY, Tokyo, Japan) with 488 nm excitation and FITC (515–545 nm) emission channels. The acquisition and analysis software on the EC800 was used to acquire and quantify the fluorescent intensities. The EC800 Flow Cytometry Analyzer provided sensitive fluorescence measurements in addition to forward and side scatter measurements. It also allowed fluorescence normalization and accurate cell volumetric measurements. As electrolytes flowed through the aperture, the resistance between the electrodes was extremely low. When a particle passed through the aperture, the volume of the electrolyte was displaced by the particle, thus increasing the impedance between the electrodes resulting in a quantifiable voltage pulse. The pulse height was directly proportional to the volume of the displaced electrolyte and the cell volume [25].

To confirm that VEGF actually increased the cellular volume of Müller cells through formation of NO, we performed an additional FACS experiment using a NO synthase inhibitor, N<sup>ω</sup>-nitro-L-arginine methyl ester (L-NAME, 1 mM).

### Statistical analyses

The means and standard error of the means were calculated. Unless noted, two-tailed Student's *t*-tests were used. The level of significance was set at  $P < 0.05$ .

## Results

### Immunohistochemistry of retinal slices

Photomicrographs of retinal sections stained immunohistochemically with anti-VEGF antibody (red) and anti-GFAP antibody (green) are shown in Fig. 1. Sections were obtained from eyes receiving intravitreal injections of (A) a vehicle or (B) VEGF in nondiabetic rats, and (C) a vehicle or (D) VEGF in STZ-induced diabetic rats. Compared with the vehicle-injected, nondiabetic rats (Fig. 1a), immunoreactivity to VEGF was increased in all other groups and highest in the VEGF-injected STZ-induced diabetic rats (Fig. 1d). Following injections of VEGF into the vitreous of nondiabetic rats (Fig. 1b), immunoreactivity to VEGF was increased in the ganglion cell layer (GCL), the inner plexiform layer (IPL), and the inner nuclear layer (INL). In the



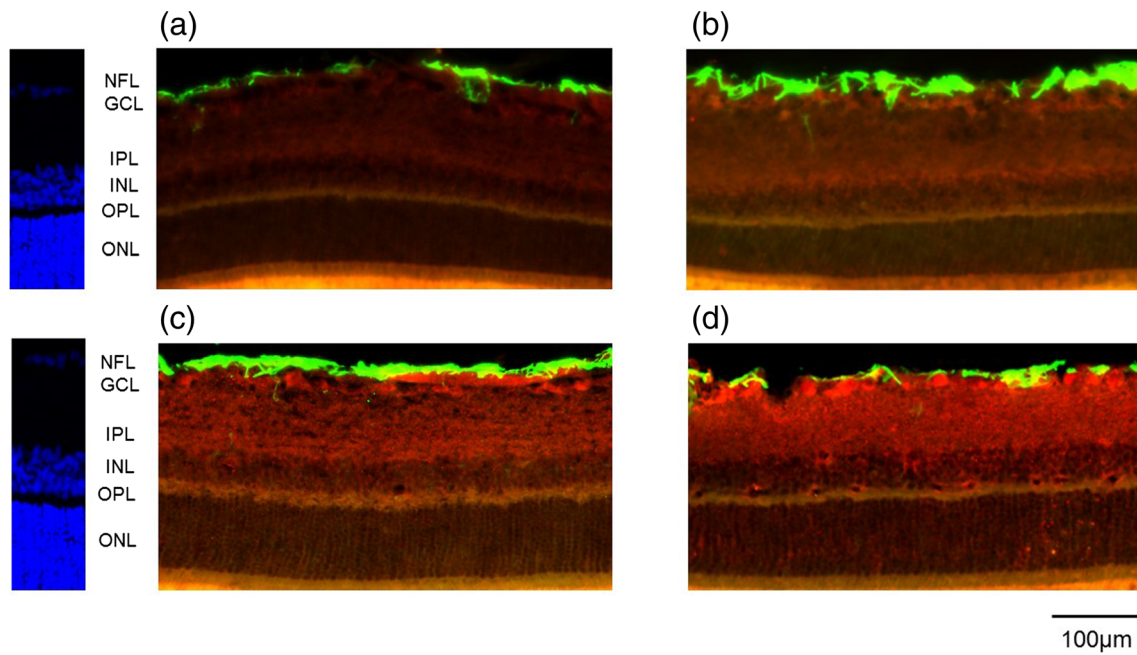


**Fig. 1** Representative photomicrographs of retinal tissues stained immunohistochemically with anti-VEGF (*red*) and anti-GFAP (*green*) antibodies. Sections were obtained from eyes receiving intravitreal injections of (a) a vehicle or (b) VEGF in normoglycemic rats, (c) a vehicle or (d) VEGF in hyperglycemic rats. Compared with the control, vehicle-injected normoglycemic rats (a), immunoreactivity to VEGF was higher

in all other groups and highest in the VEGF-injected diabetic rat retinas (d). When VEGF was injected into the vitreous of normoglycemic rats (b), immunoreactivity to VEGF was increased. In diabetic retinas, VEGF expression was more intense in the internal retinal layers (c), and further increased with VEGF injection (d)

diabetic retina, VEGF expression was intensified in these internal retinal layers (Fig. 1c), which was more intensified in the VEGF injected samples (Fig. 1d). These results suggest VEGF expression is an autoregulatory event.

Figure 2 shows retinal sections stained immunohistochemically with an anti-AQP4 antibody (*red*) and an anti-GFAP antibody (*green*). In the diabetic rat retina (Fig. 2b), immunoreactivity to AQP4 was higher than the control (Fig. 2a).

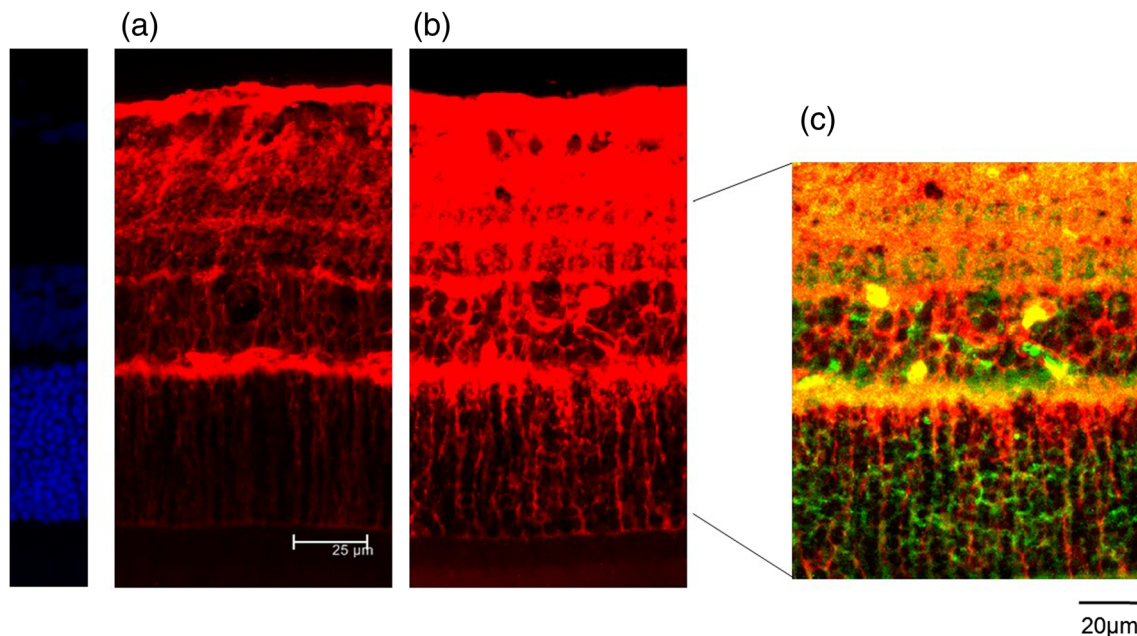


**Fig. 2** Representative photomicrographs of retina tissues stained immunohistochemically with anti-AQP4 (*red*) and anti-GFAP (*green*) antibodies. Sections were obtained from nondiabetic rats (control, a) and STZ-induced hyperglycemic rats (b). In the diabetic rat retina (b), the

immunoreactivity to AQP4 was higher than the control (a). Double staining for AQP4 and GFAP demonstrated that the expression of AQP4 was colocalized with GFAP expression in STZ-induced hyperglycemic rats (c)

**Table 1** Semi-quantification of immunofluorescence signal in each group

	(A)	(B)	(C)	(D)
VEGF	51.60	78.88	88.44	92.61
	54.83	78.66	93.69	99.15
	50.46	79.39	86.61	86.92
	mean	52.29	78.98*	89.58*
S.D.	2.27	0.38	3.67	6.12
GFAP	19.07	24.26	36.63	46.61
	17.09	22.29	35.30	47.64
	19.26	27.03	37.77	45.51
	mean	18.47	24.53*	36.57*
S.D.	1.20	2.38	1.24	1.06
AQP4	51.60	59.02	69.70	71.72
	53.53	61.30	72.62	82.38
	51.37	64.97	70.72	77.30
	mean	52.16	61.76*	71.01*
S.D.	1.18	3.00	1.48	5.34 (AIU)

Eyes receiving intravitreal injections of (A) a vehicle or (B) VEGF in normoglycemic rats, (C) a vehicle or (D) VEGF in hyperglycemic rats

\*:  $P < 0.05$  vs control (A)

Additionally, the observed longitudinal pattern of AQP4 immunoreactivity to AQP4 in the inner plexiform layer (IPL), the inner nuclear layer (INL), the outer plexiform layer (OPL), and the outer nuclear layer (ONL), suggested that AQP4 expression

was increased in the Müller cells. Double staining for AQP4 and GFAP, a glial cell marker, demonstrated that the expression of AQP4 was co-localized with GFAP expression (Fig. 2c). Semi-quantification of the immunofluorescence signals representing VEGF, GFAP, and AQP4 expression in each group was analyzed using Image J software (NIH, Bethesda, MD, Table 1).

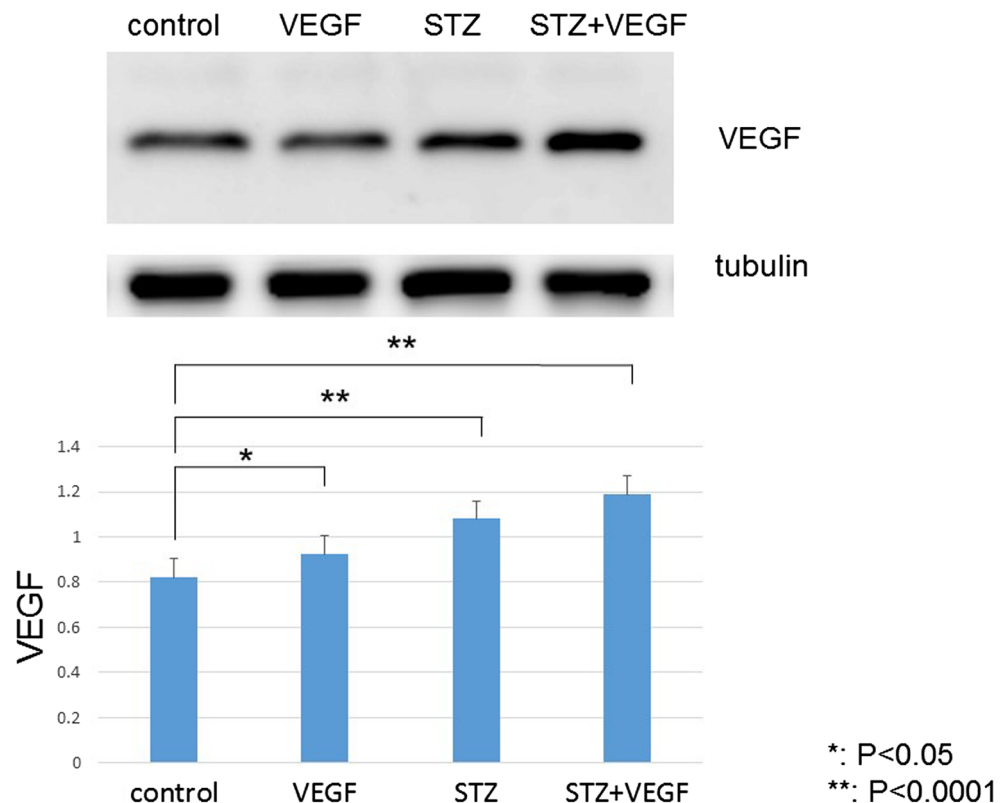
### Protein levels of VEGF in retina by western blot

Figure 3 shows VEGF protein levels in the retina as determined by western blot analysis. VEGF expression in nondiabetic rats injected with VEGF was significantly ( $P = 0.025$ ) increased by 12.3%, suggesting the existence of an autocrine loop in the formation of intraretinal VEGF [26]. Additionally, the increase of VEGF was more enhanced in STZ-induced diabetic rats. In diabetic rats, protein levels of VEGF were increased 31.5% compared to the control ( $P < 0.0001$ ), and increased 44.7% in VEGF-injected diabetic rats.

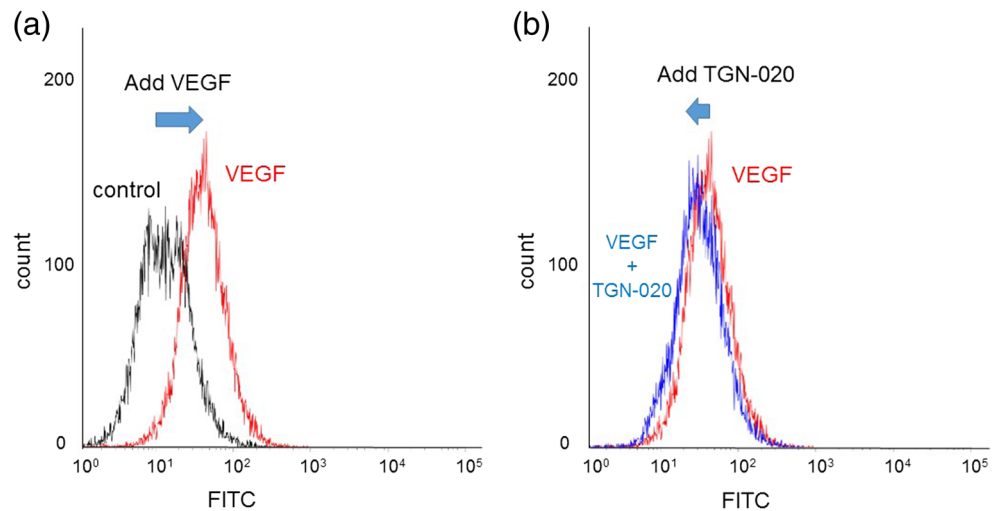
### VEGF causes Müller cell swelling

Representative graphs showing the changes of DAF-2T fluorescent intensities in cultured Müller cells (TR-MUL5) are shown in Fig. 4. DAF-2T fluorescent intensities were determined using FACS and plotted on the abscissa, while the total number of cells

**Fig. 3** Protein levels of VEGF in retinal slices by western blot analyses. Compared to the control, VEGF expression was significantly increased in retinal slices obtained from eyes receiving intravitreal injections of VEGF in normoglycemic rats. Additionally, the increased VEGF expression was more enhanced in STZ-induced hyperglycemic rats ( $P < 0.05$ )



**Fig. 4** Nitric oxide levels present in cultured Müller cells exposed to the presence or absence of VEGF and TGN-020, an AQ4 inhibitor. DAF-2T fluorescent intensities were determined using FACS and plotted on the abscissa, while the number of cells was plotted on the ordinate. The control graph (black) was shifted to the right (red) in the presence of VEGF (a); however, the control graph was shifted to the left (blue) with the administration of TGN-020, even in the presence of VEGF (b)



was plotted on the ordinate. Exposure to VEGF caused an increase of DAF-2T intensities in TR-MUL5 cells (Fig. 4a). On the other hand, DAF-2T intensities were decreased following the addition of an aquaporin 4 blocker, TGN-020 (100 nM, Fig. 4b).

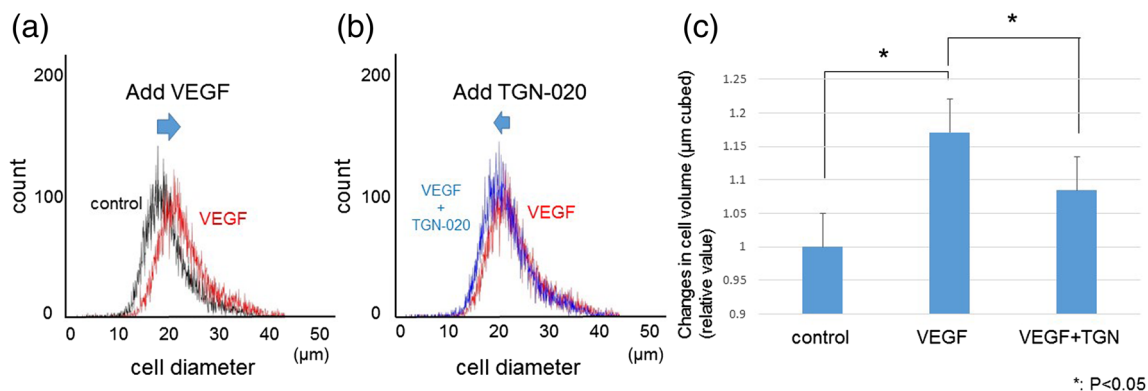
Representative graphs showing the changes in cell diameter of cultured Müller cells (TR-MUL5) are shown in Fig. 5. Cell diameter was determined using FACS and plotted on the abscissa, while the number of cells was plotted on the ordinate. Exposure to VEGF caused an increase in the cell diameter of TR-MUL5 cells (Fig. 5a). On the other hand, the increase in the cell diameter was reduced following the addition of TGN-020 (100 nM, Fig. 5b). Figure 5c shows graphs illustrating the changes in cellular volumes of TR-MUL5 cells. Based on these FACS analyses, exposure to VEGF caused an increase in cellular volume, while TGN-020 significantly ( $P < 0.05$ ) reduced the enlargement.

Figure 6 demonstrates the observed changes of DAF-2T fluorescent intensities in cultured Müller cells (TR-MUL5) exposed to L-NAME, a NO synthase inhibitor. Exposure to VEGF caused an increase of DAF-2T intensities in TR-MUL5 cells. On the

other hand, DAF-2T intensities were decreased following the addition of L-NAME. Representative graphs illustrating the changes in cell diameter of cultured Müller cells (TR-MUL5) are shown in Fig. 7. Exposure to VEGF caused an increase in the cell diameter of TR-MUL5 cells (Fig. 7a). On the other hand, the increase in the cell diameter was reduced following the addition of L-NAME (Fig. 7b). In Fig. 7c, the graphs illustrate the changes in cellular volumes of TR-MUL5 cells. Based on these FACS analyses, exposure to VEGF caused an increase in cellular volume, while L-NAME significantly ( $P < 0.05$ ) reduced this enlargement.

## Discussion

Our results showed that VEGF was increased in retinas of STZ-induced diabetic rats. VEGF caused an increase in the cellular volume of cultured Müller cells along with an increase in intracellular NO levels. Additionally, TGN-020, an AQ4 inhibitor, suppressed the VEGF-induced changes.



**Fig. 5** Graphs showing the changes in cell diameter of cultured Müller cells (TR-MUL5). Cell diameter was determined using FACS and plotted on the abscissa, while the number of cells was plotted on the ordinate. Exposure to VEGF caused an increase in the cell diameter of TR-MUL5 cells (a). On the other hand, the cell diameter was decreased with the

addition of TGN-020, an AQ4 inhibitor (b). Graphs showing cell volume changes in TR-MUL5 cells (c). According to FACS analyses, exposure to VEGF caused an increase in the cellular volume of TR-MUL5 cells, while TGN-020, an AQ4 4 inhibitor, suppressed the enlargement ( $P < 0.05$ )

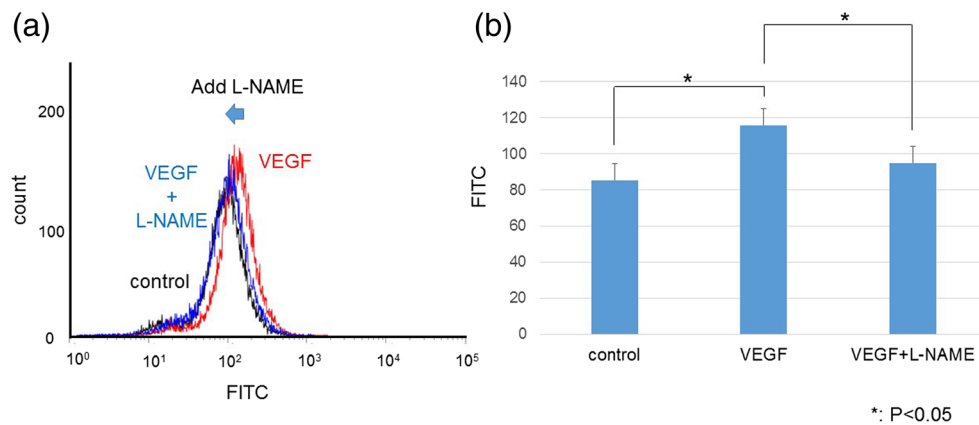


**Fig. 6** The observed changes of DAF-2T fluorescent intensities in cultured Müller cells (TR-MUL5) exposed to L-NAME, a NO synthase inhibitor. DAF-2T fluorescent intensities were determined using FACS and plotted on the abscissa, while the number of cells was plotted on the ordinate (a). Exposure to VEGF caused an increase in DAF-2T intensities

of TR-MUL5 cells. On the other hand, DAF-2T intensities were decreased following the addition of L-NAME. Graphs (b) show the significant changes in DAF-2T intensities of TR-MUL5 cells in each group ( $P < 0.05$ )

Under normal circumstances, quiescent endothelial cells secrete low levels of VEGF [27] to maintain the physiological condition of the retina [19]. On the other hand, Müller cells are also a main source of VEGF, which assists in controlling the growth of the deep plexus retinal vasculature [28]. However, once VEGF production is increased in diabetic retinopathy or ischemic retinal diseases, the increased vessel permeability results in macular edema [29]. Tolentino et al. injected VEGF into the vitreous of healthy monkey eyes, which resulted in changes similar to those seen in diabetic retinopathy, including vascular dilatation, microaneurysms, capillary closure, and retinal edema [30]. Thus, VEGF, in excess, can result in devastating effects for the retina under both diabetic and normoglycemic conditions.

Our results also showed that intravitreal injections of VEGF increased the immunoreactivities to VEGF, AQP4, and GFAP in the retina. These changes were observed in both the normoglycemic and diabetic rats, but the changes were more intense in the diabetic retinas. Because GFAP is an

intermediate filament present in both Müller cells and astrocytes, the increased GFAP expression indicates hypertrophy of these glial cells. The increased GFAP expression in Müller cells is a well-known phenomenon in the diabetic retina. Because upregulation of VEGF and GFAP is already known to occur in diabetic retinas, [31] VEGF expression is linked to these changes in glial cells of the diabetic retina.

In addition to increased blood-retinal barrier permeability, the impairment of fluid clearance from the retinal tissue may contribute to the development of retinal edema [11]. Expression of AQP4 in the retina is restricted to Müller cells and astrocytes [32]. Our results showed that AQP4 immunoreactivity was concentrated in the GCL, IPL, INL, OPL, and ONL. The expression of AQP4 was colocalized with GFAP throughout the retinal layers. The cell bodies of Müller cells are found exclusively in the inner nuclear layer with their processes spanning the entire length of the retina [33]. Although astrocytes are known to exist in the ganglion cell layer, the longitudinal expression pattern suggests the

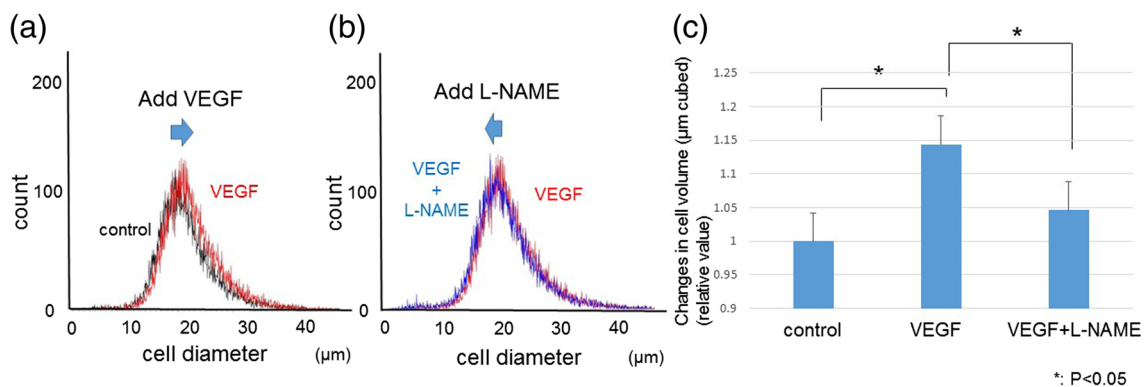


**Fig. 7** Representative graphs showing the changes in cell diameter of cultured Müller cells (TR-MUL5). Exposure to VEGF caused an increase in the cell diameter of TR-MUL5 cells (a). On the other hand, the increase in the cell diameter was reduced following the addition of L-NAME (b).

Graphs (c) show the changes in cellular volumes of TR-MUL5 cells. Based on these FACS analyses, exposure to VEGF caused an increase in cellular volume, while L-NAME significantly ( $P < 0.05$ ) reduced the enlargement



upregulation of these proteins involves Müller cells. In a previous study, Qin et al. [34] showed that AQP4 was mainly expressed in the end feet of Müller cells from STZ-induced diabetic rats. We showed that AQP4 was also highly expressed in both the end feet and cell bodies of Müller cells from STZ-induced diabetic rats. One difference between the two studies was that they used eight-week-old Wistar Kyoto rats one week after STZ injection, while we used nine-week-old Wistar rats 2 weeks after the induction of diabetes.

It is already known that the expression of AQP4 in Müller cells has a polarized distribution with predominant expression located at the end foot processes facing the vitreous body or capillary endothelium. They are also responsible for the transport of water that accumulates in the tissue as the end product of ATP synthesis [10]. Using wild-type and AQP4 knockout mice, Da and Verkman investigated the role AQP4 may play in altering retinal Müller cells exposed to ischemic conditions following retinal injury. They found that AQP4 deletion in mice is neuroprotective in a transient ischemia model of retinal injury [15]. Müller cells are thought to play a role in water handling in the retina by directing osmotically driven water flux to the vitreous and vessels. Thus, we focused on the Müller cells and investigated whether the inhibition of AQP4 could suppress the swelling of retinal Müller cells under osmotic challenges.

Blocking the production of NO by L-NAME reduced VEGF-induced cell swelling as shown in Figs. 6 and 7. Results from our *in vitro* assay suggested that VEGF actually increased the cellular volume of Müller cells through the formation of NO. This finding is in agreement with our previous finding that NO increases the expression of AQP4 protein, [35] and the enlargement of optic nerve astrocytes. Other reports showed that VEGF induces NO formation, which then activates the transcription of VEGF [36, 37]. Because TGN-020, a specific blocker of the AQP4 channel, reduced the VEGF-induced increases of NO and cellular volume, the actions of VEGF are, in part, mediated through the AQP4 channel.

In our FACS study, the fluorescent intensity of DAF-2T was increased following the addition of VEGF to cultured Müller cells, and the increase was suppressed by TGN-020, as shown in Fig. 4. These findings suggested that VEGF induced NO formation in Müller cells, while the VEGF-induced increase of NO was suppressed by TGN-020, a selective AQP4 inhibitor. Other reports demonstrated that NO increases the expression of AQP4 protein [35]. Thus, the enlargement of Müller cells seen in our study (Fig. 5) was likely due to AQP4 and VEGF, but confirming our findings using primary-cultured Müller cells would be informative.

There are some limitations in this study. One limitation of our study is that our results were obtained from normoglycemic and STZ-induced hyperglycemic rats, which have no macula. Thus, direct links of our findings to human diabetic macular edema should be considered cautiously. It will be important to

confirm the present results using mammals that possess a macula, such as monkeys. Second, we performed an *in vitro* study using a rat retinal Müller cell line to assess the involvement of VEGF-induced NO production in retinal Müller cells. To confirm these data, similar experiments should be performed using primary isolated Müller cells from both normoglycemic and STZ-induced hyperglycemic rats.

In conclusion, our findings from *in vivo* and *in vitro* experiments showed that excess VEGF induces Müller cell swelling through the formation of NO and AQP4 channels. Thus, AQP4 channels may be a target for the treatment of diabetic retinal edema and the associated Müller cell swelling.

**Acknowledgements** The authors thank English Manuscript Editors, LLC for editorial assistance.

**Publisher's Note** Springer Nature remains neutral with regard to jurisdictional claims in published maps and institutional affiliations.

#### Compliance with ethical standards

**Funding** Grant-in-Aid for Scientific Research (C) (Researcher No. 90610105) from the Japan Society for the Promotion of Science (Tokyo, Japan), and the Osaka Eye Bank Association Fund (Osaka, Japan) provided financial support. The sponsor had no role in the design or conduct of this research.

**Conflict of interest** All authors certify that they have no affiliations with or involvement in any organization or entity with any financial interest (such as honoraria; educational grants; participation in speakers' bureaus; membership, employment, consultancies, stock ownership, or other equity interest; and expert testimony or patent-licensing arrangements), or non-financial interest (such as personal or professional relationships, affiliations, knowledge or beliefs) in the subject matter or materials discussed in this manuscript.

**Ethical approval (Animal experiments)** All applicable guidelines of ARVO Statement for the care and use of animals were followed. Our experimental protocols conformed to the Animal Research: Reporting In Vivo Experiments (ARRIVE) guidelines.

All procedures performed in studies involving animals were in accordance with the ethical standards of the Osaka Medical College Committee on the Use and Care of Animals (Approval number: 27114) at which the studies were conducted.

#### References

- Whitmire W, Al-Gayyar MM, Abdelsaid M, Yousufzai BK, El-Remessy AB (2011) Alteration of growth factors and neuronal death in diabetic retinopathy: what we have learned so far. *Mol Vis* 17:300–308
- Busch S, Kannt A, Kolibabka M, Schlotterer A, Wang Q, Lin J, Feng Y, Hoffmann S, Gretz N, Hammes HP (2014) Systemic treatment with erythropoietin protects the neurovascular unit in a rat model of retinal neurodegeneration. *PLoS One* 9:e102013. doi:10.1371/journal.pone.0102013
- Bandello F, Tejerina AN, Vujosevic S, Varano M, Egan C, Sivaprasad S, Menon G, Massin P, Verbraak FD, Lund-Andersen H, Martinez JP, Jurgens I, Smets RM, Coriat C, Wiedemann P,



- Agoas V, Querques G, Holz FG, Nunes S, Alves D, Neves C, Santos T, Ribeiro L, Cunha-Vaz J, Evicr.net (2015) Retinal layer location of increased retinal thickness in eyes with subclinical and clinical macular edema in diabetes type 2. *Ophthalmic Res* 54:112–117. doi:10.1159/000438792
4. Klaassen I, Van Noorden CJ, Schlingemann RO (2013) Molecular basis of the inner blood-retinal barrier and its breakdown in diabetic macular edema and other pathological conditions. *Prog Retin Eye Res* 34:19–48. doi:10.1016/j.preteyeres.2013.02.001
  5. Das A, McGuire PG, Rangasamy S (2015) Diabetic macular edema: pathophysiology and novel therapeutic targets. *Ophthalmology* 122:1375–1394. doi:10.1016/j.ophtha.2015.03.024
  6. Ferrara N (2016) VEGF and intraocular neovascularization: from discovery to therapy. *Transl Vis Sci Technol* 5:10. doi:10.1167/tvst.5.2.10
  7. Lally DR, Shah CP, Heier JS (2016) Vascular endothelial growth factor and diabetic macular edema. *Surv Ophthalmol*. doi:10.1016/j.survophthal.2016.03.010
  8. Aiello LP, Beck RW, Bressler NM, Browning DJ, Chalam KV, Davis M, Ferris FL 3rd, Glassman AR, Maturi RK, Stockdale CR, Topping TM (2011) Rationale for the diabetic retinopathy clinical research network treatment protocol for center-involved diabetic macular edema. *Ophthalmology* 118:e5–e14. doi:10.1016/j.ophtha.2011.09.058
  9. Bringmann A, Pannicke T, Grosche J, Francke M, Wiedemann P, Skatchkov SN, Osborne NN, Reichenbach A (2006) Muller cells in the healthy and diseased retina. *Prog Retin Eye Res* 25:397–424. doi:10.1016/j.preteyeres.2006.05.003
  10. Nielsen S, Nagelhus EA, Amiry-Moghaddam M, Bourque C, Agre P, Ottersen OP (1997) Specialized membrane domains for water transport in glial cells: high-resolution immunogold cytochemistry of aquaporin-4 in rat brain. *J Neurosci* 17:171–180
  11. Bringmann ARA, Wiedemann P (2004) Pathomechanisms of cystoid macular edema. *Ophthalmic Res* 36:241–249
  12. Goodyear MJ, Crewther SG, Junghans BM (2009) A role for aquaporin-4 in fluid regulation in the inner retina. *Vis Neurosci* 26:159–165. doi:10.1017/s0952523809090038
  13. Spaide RF (2016) Retinal vascular cystoid macular edema: review and new theory. *Retina*. doi:10.1097/iae.0000000000001158
  14. Papadopoulos MC, Verkman AS (2007) Aquaporin-4 and brain edema. *Pediatr Nephrol* 22:778–784. doi:10.1007/s00467-006-0411-0
  15. Da T, Verkman AS (2004) Aquaporin-4 gene disruption in mice protects against impaired retinal function and cell death after ischemia. *Invest Ophthalmol Vis Sci* 45:4477–4483. doi:10.1167/iovs.04-0940
  16. Wang Y, Tajkhorshid E (2010) Nitric oxide conduction by the brain aquaporin AQP4. *Proteins* 78:661–670. doi:10.1002/prot.22595
  17. Gunnarson E, Zelenina M, Axehult G, Song Y, Bondar A, Krieger P, Brismar H, Zelenin S, Aperia A (2008) Identification of a molecular target for glutamate regulation of astrocyte water permeability. *Glia* 56:587–596. doi:10.1002/glia.20627
  18. Plate KH, Breier G, Risau W (1994) Molecular mechanisms of developmental and tumor angiogenesis. *Brain Pathol* 4:207–218
  19. Ferrara N, Davis-Smyth T (1997) The biology of vascular endothelial growth factor. *Endocr Rev* 18:4–25. doi:10.1210/edrv.18.1.0287
  20. Kilkenny C, Browne WJ, Cuthill IC, Emerson M, Altman DG (2010) Improving bioscience research reporting: the ARRIVE guidelines for reporting animal research. *PLoS Biol* 8:e1000412. doi:10.1371/journal.pbio.1000412
  21. Tomi M, Funaki T, Abukawa H, Katayama K, Kondo T, Ohtsuki S, Ueda M, Obinata M, Terasaki T, Hosoya K (2003) Expression and regulation of L-cystine transporter, system xc<sup>-</sup>, in the newly developed rat retinal Muller cell line (TR-MUL). *Glia* 43:208–217. doi:10.1002/glia.10253
  22. Obinata M (2007) The immortalized cell lines with differentiation potentials: their establishment and possible application. *Cancer Sci* 98:275–283. doi:10.1111/j.1349-7006.2007.00399.x
  23. Vogler S, Grosche A, Pannicke T, Wiedemann P, Reichenbach A, Bringmann A (2016) Endothelins inhibit osmotic swelling of rat retinal glial and bipolar cells by activation of growth factor signaling. *Neurochem Res*. doi:10.1007/s11064-016-1971-4
  24. Hoffman RA, Johnson TS, Britt WB (1981) Flow cytometric electronic direct current volume and radiofrequency impedance measurements of single cells and particles. *Cytometry* 1:377–384. doi:10.1002/cyto.990010605
  25. Potapova TA, Seidel CW, Box AC, Rancati G, Li R (2016) Transcriptome analysis of tetraploid cells identifies cyclin D2 as a facilitator of adaptation to genome doubling in the presence of p53. *Mol Biol Cell* 27:3065–3084. doi:10.1091/mbc.E16-05-0268
  26. Klettner A, Westhues D, Lassen J, Bartsch S, Roider J (2013) Regulation of constitutive vascular endothelial growth factor secretion in retinal pigment epithelium/choroid organ cultures: p38, nuclear factor kappaB, and the vascular endothelial growth factor receptor-2/phosphatidylinositol 3 kinase pathway. *Mol Vis* 19:281–291
  27. Carmeliet P, Jain RK (2011) Molecular mechanisms and clinical applications of angiogenesis. *Nature* 473:298–307. doi:10.1038/nature10144
  28. Stone J, Itin A, Alon T, Pe'er J, Gnessin H, Chan-Ling T, Keshet E (1995) Development of retinal vasculature is mediated by hypoxia-induced vascular endothelial growth factor (VEGF) expression by neuroglia. *J Neurosci* 15:4738–4747
  29. Viores SA, Youssri AI, Luna JD, Chen YS, Bhargava S, Viores MA, Schoenfeld CL, Peng B, Chan CC, LaRochelle W, Green WR, Campochiaro PA (1997) Upregulation of vascular endothelial growth factor in ischemic and non-ischemic human and experimental retinal disease. *Histol Histopathol* 12:99–109
  30. Tolentino MJ, Miller JW, Gragoudas ES, Jakobiec FA, Flynn E, Chatzistefanou K, Ferrara N, Adamis AP (1996) Intravitreal injections of vascular endothelial growth factor produce retinal ischemia and microangiopathy in an adult primate. *Ophthalmology* 103:1820–1828
  31. Mancini JE, Ortiz G, Croxatto JO, Gallo JE (2013) Retinal upregulation of inflammatory and proangiogenic markers in a model of neonatal diabetic rats fed on a high-fat-diet. *BMC Ophthalmol* 13:14. doi:10.1186/1471-2415-13-14
  32. Schey KL, Wang Z, J LW, Qi Y (2014) Aquaporins in the eye: expression, function, and roles in ocular disease. *Biochim Biophys Acta* 1840:1513–1523. doi:10.1016/j.bbagen.2013.10.037
  33. Newman E, Reichenbach A (1996) The Muller cell: a functional element of the retina. *Trends Neurosci* 19:307–312
  34. Qin Y, Ren H, Hoffman MR, Fan J, Zhang M, Xu G (2012) Aquaporin changes during diabetic retinopathy in rats are accelerated by systemic hypertension and are linked to the renin-angiotensin system. *Invest Ophthalmol Vis Sci* 53:3047–3053. doi:10.1167/iovs.11-9154
  35. Oku H, Morishita S, Horie T, Kida T, Mimura M, Fukumoto M, Kojima S, Ikeda T (2015) Nitric oxide increases the expression of aquaporin-4 protein in rat optic nerve astrocytes through the cyclic guanosine monophosphate/protein Kinase G pathway. *Ophthalmic Res* 54:212–221. doi:10.1159/000440846
  36. Kruzliak P, Novak J, Novak M (2014) Vascular endothelial growth factor inhibitor-induced hypertension: from pathophysiology to prevention and treatment based on long-acting nitric oxide donors. *Am J Hypertens* 27:3–13. doi:10.1093/ajh/hpt201
  37. Shen BQ, Lee DY, Zioncheck TF (1999) Vascular endothelial growth factor governs endothelial nitric-oxide synthase expression via a KDR/Flk-1 receptor and a protein kinase C signaling pathway. *J Biol Chem* 274:33057–33063